

Supporting Information

Bimetallic alloy nanocrystals encapsulated in ZIF-8 for synergistic catalysis of ethylene oxidation degradation

Yuanbiao Huang, Yaohong Zhang, Xuxing Chen, Dongshuang Wu, Zhiguo Yi,

Rong Cao*

Materials

ZIF-8 was synthesized according to the public literature.^[1] All other reagents were commercial purchased and used as received.

Characterization

Analysis of noble metal content was measured by inductively coupled plasma atomic emission spectroscopy (ICP-AES) on an Ultima 2 analyzer (Jobin Yvon). Powder X-ray diffraction (PXRD) patterns were recorded on a Rigaku-Dmax2500 diffractometer using CuK α radiation ($\lambda = 0.154$ nm). The BET surface area measurements and ethylene sorption isotherms were performed on a Micromeritics ASAP 2010 instrument. The morphologies of catalysts were studied using a JEOL-2010 transmission electron microscope (TEM) working at 200 KV. The samples were prepared by placing a drop of product in ethanol onto a continuous carbon-coated copper TEM grid. X-ray photoelectron spectroscopy (XPS) measurements were performed on a Kratos Axis Ultra DLD system with a base pressure of 10⁻⁹ Torr.

Synthesis of PtPd alloy nanocrystals

The cubic PtPd alloy nanocrystals (NCs) were prepared according to the literature using solvothermal method.^[2] In a typical synthesis of cubic PtPd NCs, potassium tetrachloroplatinate aqueous solution (20 mM, 1.0 mL), sodium tetrachloropalladate aqueous solution (20 mM, 1.0 mL), sodium iodide (NaI, 75.0 mg) and poly(vinylpyrrolidone) (PVP, 160.0 mg) were mixed together with 10 mL N, N-dimethylformamide in a 20.0-mL vial. After the mixture was ultrasonicated for about 10 minutes, it was transferred into a conventional oven and heated at 130 °C for 5 hours. The resulting colloidal products were obtained by centrifugation and washed several times with an ethanol-acetone mixture (1:4, v/v).

Synthesis of Pt and Pd nanocrystals

The monmetallic Pt and Pd NCs were synthesized in a similar procedure of preparation of cubic PtPd alloy nanocrystals using potassium tetrachloroplatinate aqueous solution and sodium tetrachloropalladate aqueous solution, respectively.

Synthesis of PtPd@ZIF-8

Typically, 5 ml solution of 2-methylimidazole (30 mM), 1 ml PtPd NCs methanol solution of desired concentration, and 5 ml solution of $\text{Zn}(\text{NO}_3)_2 \cdot \text{H}_2\text{O}$ (30 mM) were mixed and then allowed to stand at room temperature for 24 hours without stirring. The product was collected by centrifugation, washed several times with methanol, and vacuum-dried overnight.

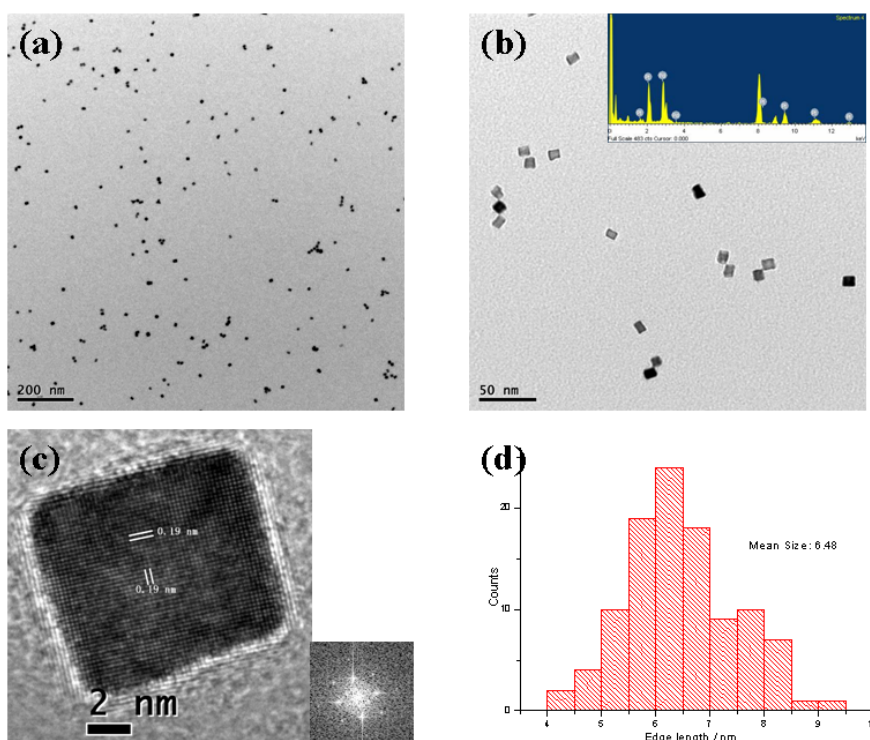
Synthesis of Pt@ZIF-8 and Pd@ZIF-8

Pt@ZIF-8 and Pd@ZIF-8 were synthesized in a similar procedure of preparation of PtPd@ZIF-8 using Pt and Pd NCs methanol solution of desired concentration,

respectively.

Ethylene conversion

Photocatalytic oxidation of C_2H_4 was examined upon PtPd@ZIF-8 samples in a fixed-bed photoreactor. The catalyst (100 mg) was spread on the flat bottom of the reactor (450 ml). The reaction gas, a mixture of C_2H_4 (45 μ L, 100 ppm) and O_2 (5 ml), was introduced into the reactor after removing the air in the cell by N_2 carrier for 20 min. The reaction was carried out without heating at atmospheric pressure upon photoirradiation from a 300 W xenon lamp located at ca. 15 cm away from the catalyst surface. At certain time intervals, the products in the gaseous phase were sampled and analyzed by gas chromatography (Fuli Instrument GC9720). The C_2H_4 conversions ($X_{C_2H_4}$) were calculated as follows: $\chi_{C_2H_4} = ([C_2H_4]_{in} - [C_2H_4]_{out}) / [C_2H_4]_{in} \times 100$ (%), where $[C_2H_4]_{in}$ and $[C_2H_4]_{out}$ is the concentration of C_2H_4 introduced to the reactor and that detected after the reactor, respectively.



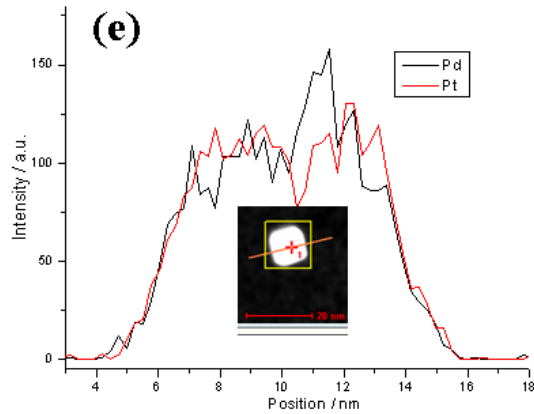


Fig. S1. (a,b) Representative TEM and HRTEM images (c) of Pt₅Pd₅ nanocrystal; (d) Edge length distribution of Pt₅Pd₅ NCs; (e) Line-scanning profile across a cubic Pt₅Pd₅ NCs, which is indicated in the inset of (e). The inset of (b) shows the energy-dispersive X-ray spectroscopy (EDS) pattern. Inset in (c) is the FFT pattern of an individual crystal.

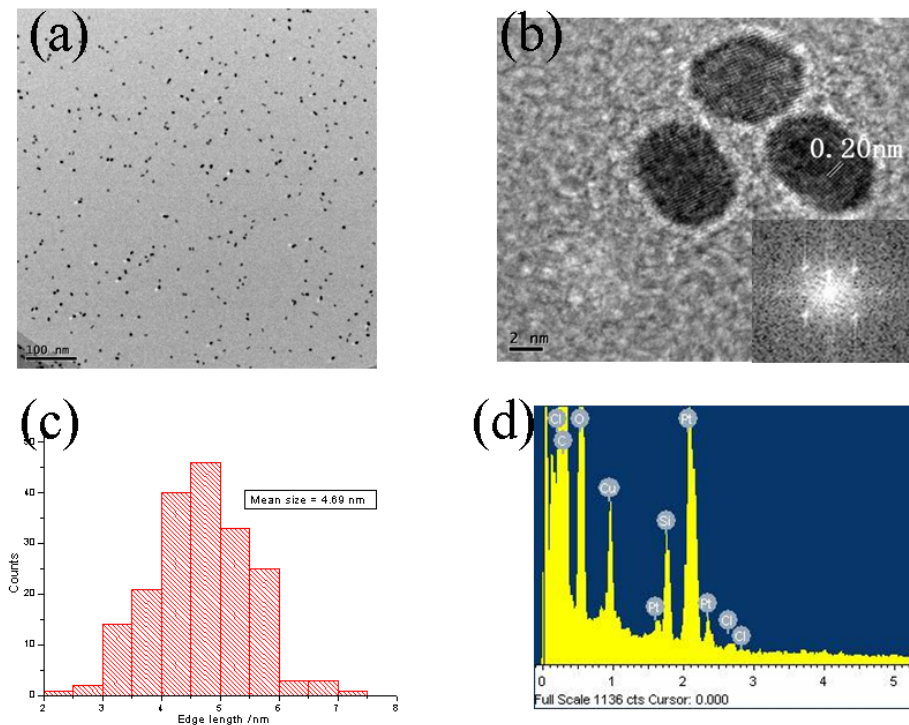


Fig. S2. (a) Representative TEM and HRTEM images (b) of cubic Pt nanocrystal; (c)

Edge length distribution of Pt NCs; (d) the energy-dispersive X-ray spectroscopy (EDS) pattern. Inset in (b) is the FFT pattern of an individual crystal.

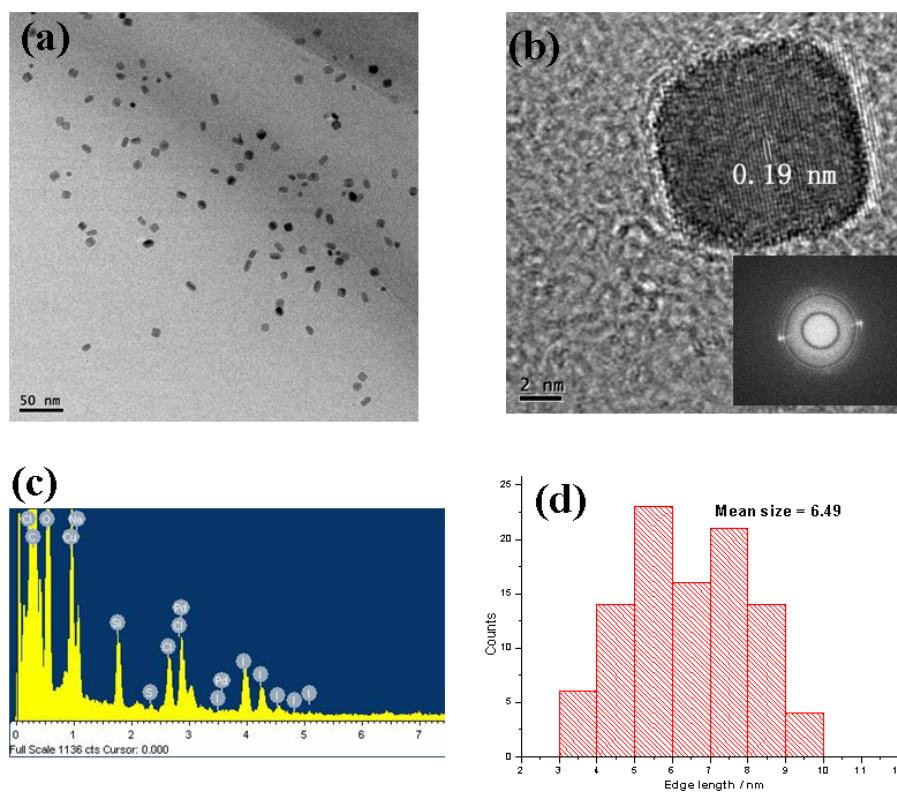


Fig. S3. (a) Representative TEM and HRTEM images (b) of cubic Pd nanocrystal; (c) the energy-dispersive X-ray spectroscopy (EDS) pattern. (d) Edge length distribution of Pd NCs; Inset in (b) is the FFT pattern of an individual crystal.

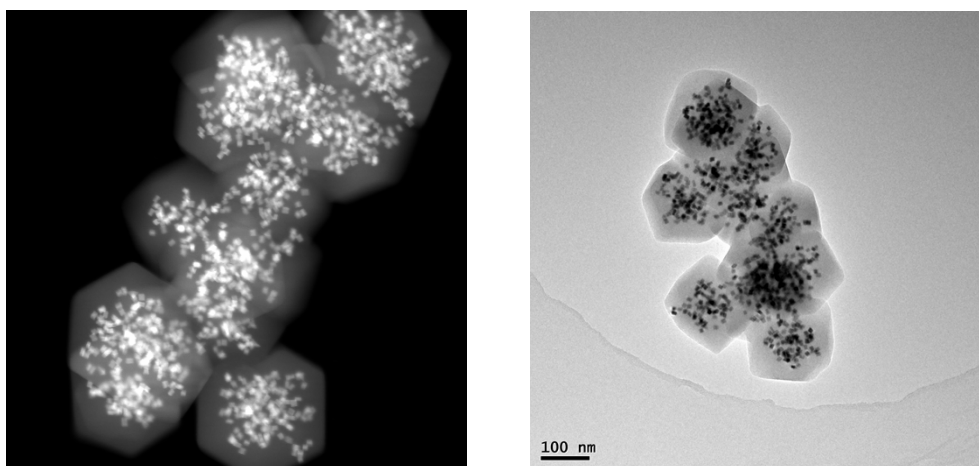


Fig. S4. (left) Dark-field TEM images of $\text{Pt}_5\text{Pd}_5@\text{ZIF-8}$; (right) TEM images of $\text{Pt}_5\text{Pd}_5@\text{ZIF-8}$ after 10 catalysis cycles.

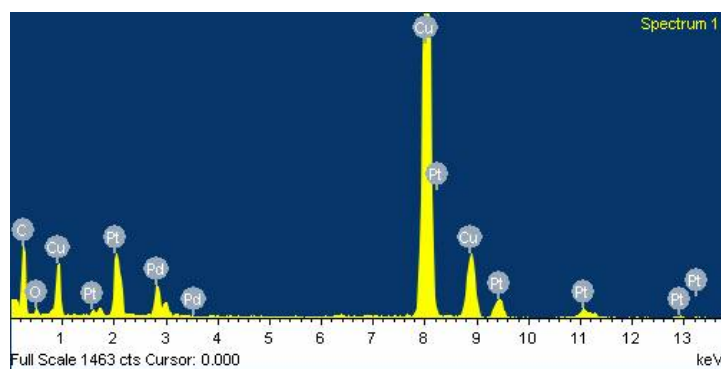


Fig. S5. The energy-dispersive X-ray spectroscopy (EDS) pattern $\text{Pt}_5\text{Pd}_5@\text{ZIF-8}$

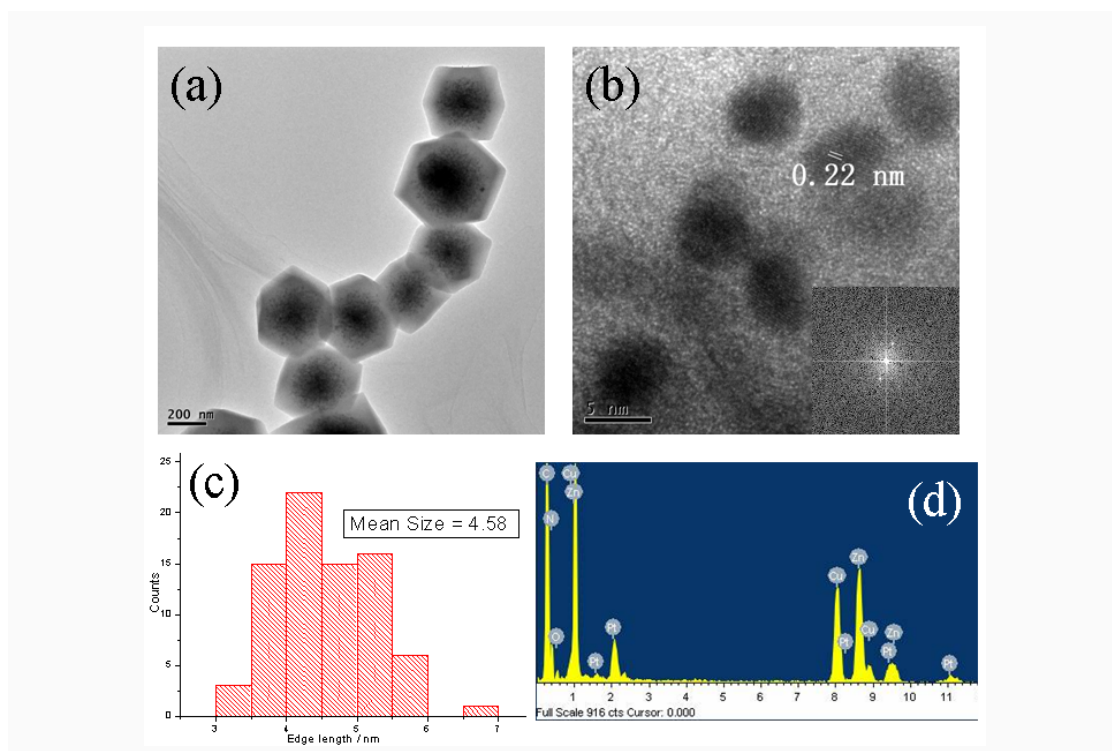


Fig. S6. (a) Representative TEM and HRTEM (b) images of Pt@ZIF-8; (c) Edge length distribution of Pt@ZIF-8; (d) The EDS pattern of Pt@ZIF-8. Inset in (b) is the FFT pattern of an individual Pt NCs.

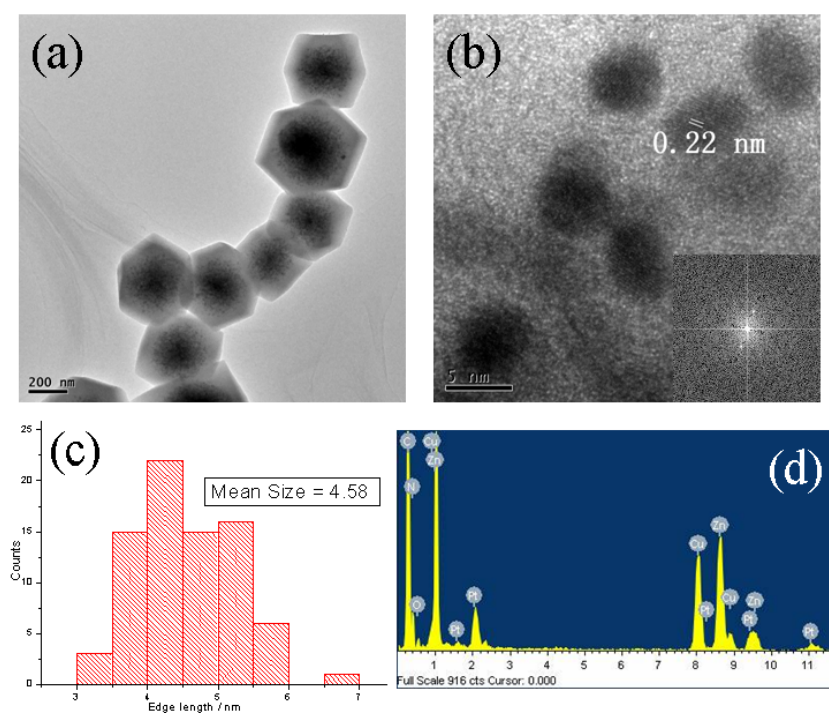


Fig. S7. (a) Representative TEM and HRTEM (b) images of Pd@ZIF-8; (c) Edge length distribution of Pd@ZIF-8; (d) The EDS pattern of Pd@ZIF-8. Inset in (b) is the FFT pattern of an individual Pd NCs.

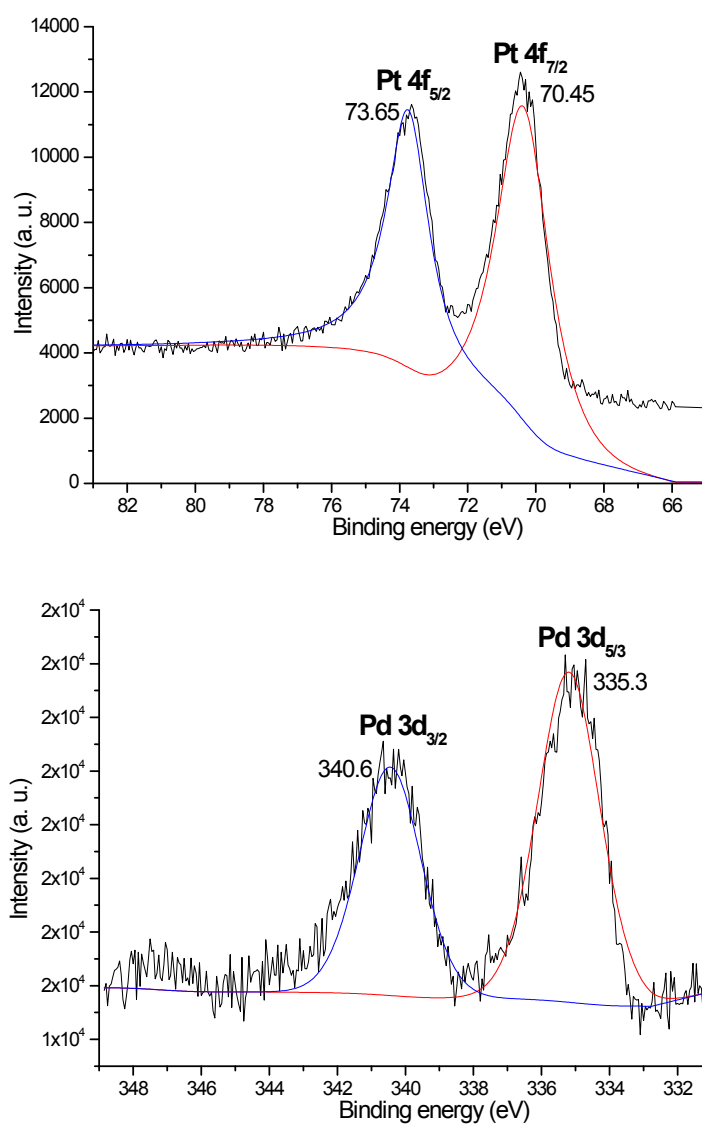


Fig. S8. XPS spectra of Pt₅Pd₅@ZIF-8 sample.

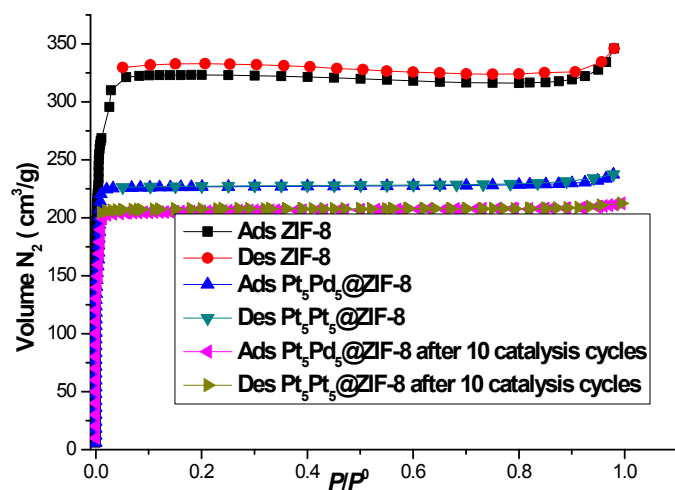


Fig. S9. Nitrogen sorption isotherms of Pt₅Pd₅@ZIF-8 (fresh and after 10 catalysis cycles) and ZIF-8 at 77 K.

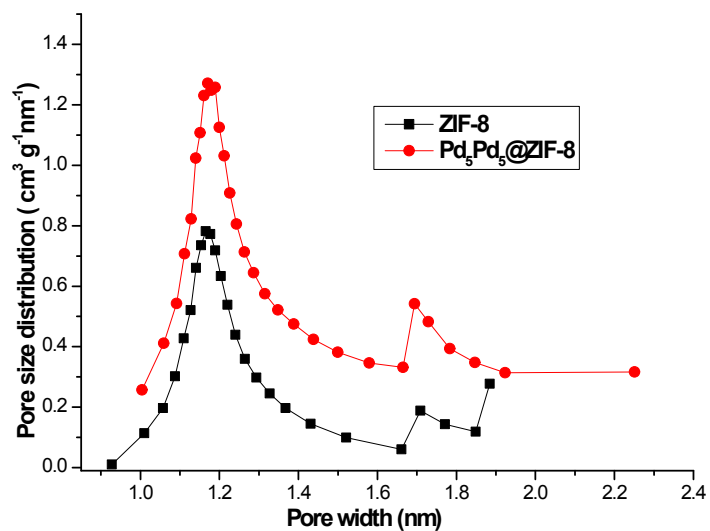


Fig. S10. Pore-size distributions of Pt₅Pd₅@ZIF-8 and ZIF-8 calculated by the Horvath-Kawazoe method

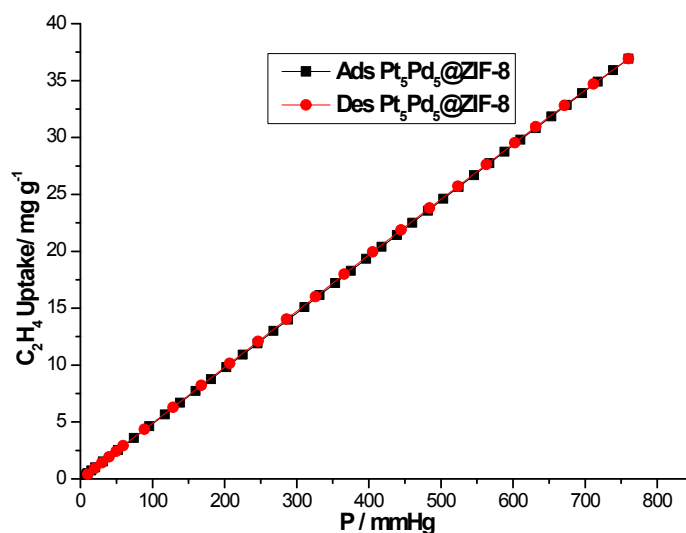


Fig. S11. Ethylene sorption isotherms of $\text{Pt}_5\text{Pd}_5@ZIF-8$ at 298 K.

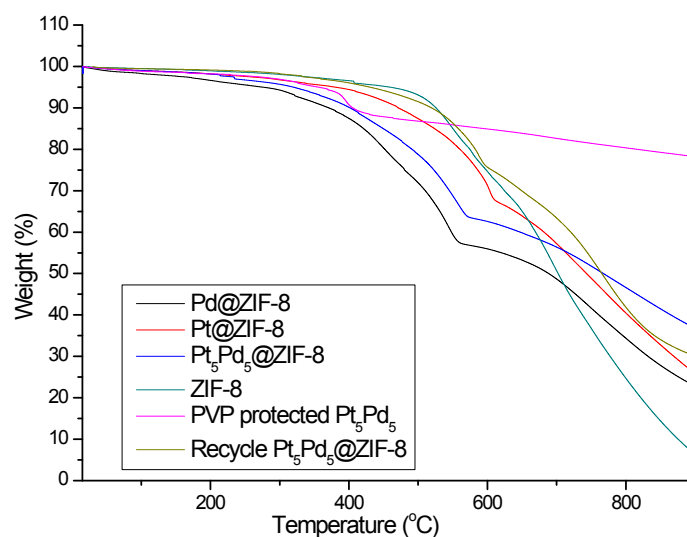


Fig. S12. Thermogravimetric analysis (TGA) curves of ZIF-8, $\text{Pt}_5\text{Pd}_5@ZIF-8$, recycled $\text{Pt}_5\text{Pd}_5@ZIF-8$ after ten cycles, $\text{Pt}@ZIF-8$ and $\text{Pd}@ZIF-8$ and catalysis in nitrogen. The results show that nanoparticle/ZIF-8 composites are less thermally stable than pure ZIF-8, perhaps because of PVP chain movement and decomposition.^[3]

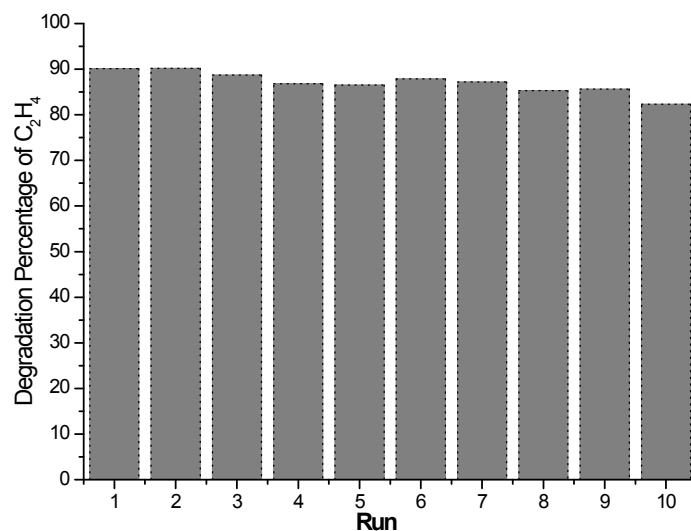


Fig. S13. Recycling test for the photocatalytic degradation of C₂H₄ under sunlight
 Conditions: 50 mg catalyst; C₂H₄: 100 ppm; O₂: 1.11×10⁴ ppm; N₂ : balance;
 Temperature, 25 °C; Time: 2 h; Xenon lamp, 300 W.

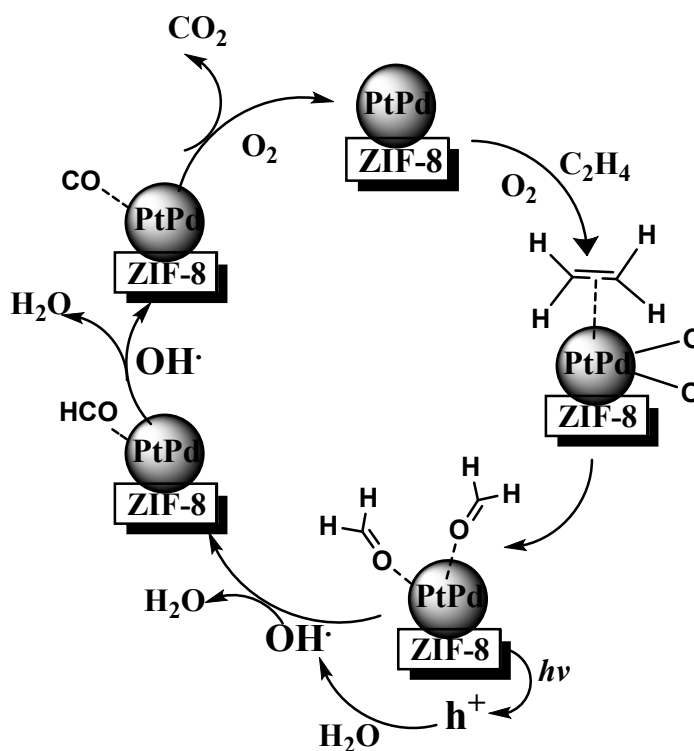


Fig. S14. Proposed mechanism of the photocatalytic degradation of ethylene by PtPd@ZIF-8

Although several studies dealing with the photocatalytic degradation of ethylene under UV irradiance have been reported in the literatures (Keller, N.; Ducamp, M.-N.; Robert, D.; Keller, V. *Chem. Rev.* **2013**, *113*, 5029), there is still uncertainty about the reaction mechanism. It was difficult to establish a mechanism of ethylene degradation

from experimental results. According to the literatures (Jiang, C.; Hara, K.; Fukuoka, A. *Angew. Chem. Int. Ed.* **2013**, *52*, 6265; Hauchecorne, B.; Tytgata, T.; Verbruggen, S. W.; Hauchecorne, D.; Terrensa, D.; Smitsa, M.; Vinken, K.; Lenaerts, S. *Appl. Catal. B: Envir.* **2011**, *105*, 111–116) and our catalysis result, we have proposed mechanism of the photocatalytic degradation of ethylene by PtPd@ZIF-8 (Fig. S14). The adsorbed C₂H₄ and O₂ react quickly to form HCHO. HCHO adsorbed on Pt is then decomposed mainly into CO₂ and H₂O in the presence of OH· radical.

Reference

- (1) R. Banerjee, A. Phan, B. Wang, C. Knobler, H. Furukawa, M. O'Keeffe, O. M. Yaghi, *Science*, **2008**, *319*, 939.
- (2) X. Huang, Y. Li, Y. Li, H. Zhou, X. Duan, Y. Huang, *Nano Lett.* **2012**, *12* (8), 4265.
- (3) G. Lu, S. Li, Z. Guo, O. K. Farha, B. G. Hauser, X. Qi, Y. Wang, X. Wang, S. Han, X. Liu, J. S. DuChene, H. Zhang, Q. Zhang, X. Chen, J. Ma, S. C. J. Loo, W. D. Wei, Y. Yang, J. T. Hupp, F. Huo, *Nature Chem.* **2012**, *19*, 1272.